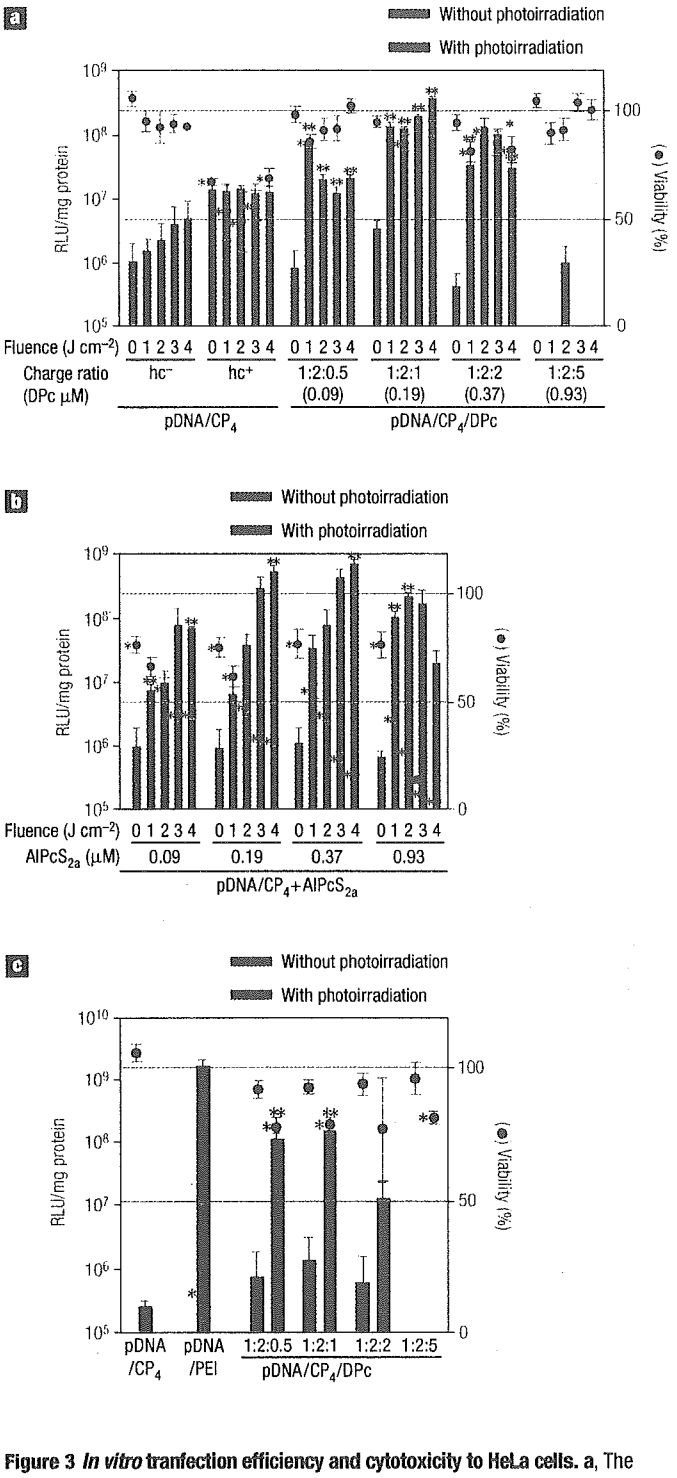

Figure 3 *In vitro* tranfection efficiency and cytotoxicity to HeLa cells. a, The effect of fluence on the transfection efficiency (bars) and photocytotoxicity (dots) of the pDNA/CP_4 and pDNA/CP_4/DPc complexes. Photoirradiation was performed 6 h after incubation with each complex, followed by 48 h post-incubation in a fresh medium. The hc represents hydroxychloroquine. **b**, The effect of fluence on the transfection efficiency (bars) and photocytotoxicity (dots) of the pDNA/CP_4 complex with different concentrations of $AlPcS_{2a}$. The same experimental conditions as **a** were applied. **c**, The transfection efficiency (bars) and photocytotoxicity (dots) when HeLa cells were irradiated 6 h after incubation with each complex at 3.6 J cm^{-2}, followed by 48 h post-incubation without medium replacement. Results are expressed as mean ± s.d. ($n = 4$). The unpaired *t*-test was used for statistical analysis, and significant changes in the cell viability (treated to untreated) and the transfection efficiency (photoirradiated to non-photoirradiated) are indicated by asterisks * and **, respectively.

PCI is a smart concept, which allows the cytoplasmic delivery of macromolecular compounds in a light-inducible manner. In previous studies, it was demonstrated that $AlPcS_{2a}$ and $TPPS_{2a}$ (meso-tetraphenylporphine with two sulphonate groups on adjacent phenyl rings) were effective in PCI-mediated delivery[8–10]. It is assumed that a hydrophobic moiety in these dissymmetric compounds may provide preferable interaction with cell membranes, whereas they are internalized by endocytosis because of high water solubility. However, such an amphiphilic nature of the compounds should generate interaction with the plasma membrane to some extent, possibly photodamaging the plasma membrane. Meanwhile, such amphiphilic photosensitizers may relocalize to some cytoplasmic organelles such as mitochondria and endoplasmic reticulum during the photoirradiation[11,22,23]. It is known that the plasma membrane and some cytoplasmic organelles might be susceptible to the photocytotoxicity[11]. These effects may be a major cause of the photocytotoxicity of $AlPcS_{2a}$ and $TPPS_{2a}$. These compounds are still useful in PCI; however, reduced photocytotoxicity might be desired in before considering further applications of this technology. We assume that the selective photodamage of the endosomal membrane is a key to reduced photocytotoxicity in PCI, motivating us to develop different gene carriers based on the PCI concept.

To design gene carriers based on the PCI concept, the following points should be considered. (i) For *in vivo* applications, the photosensitizing units should be integrated into gene carriers as one component, because separate administration of photosensitizers might result in their diffused localization to the surrounding tissues, which may decrease the efficiency in the PCI-mediated gene delivery and cause the phototoxicity to the surrounding tissues. (ii) Following internalization by the endocytosis, the photosensitizers should be released from gene carriers, otherwise, pDNA could be photochemically inactivated on photoirradiation. (iii) The photosensitizers should have increased affinity for cell membranes under endosomal conditions to accomplish the photochemical rupture of the endosomal membrane. In the ternary complex system, it was suggested that DPc may be released from the ternary complex to interact with the endosomal membrane (Fig. 2b), with the ternary complex being formed electrostatically under physiological pH conditions (Table 1), satisfying the aforementioned points for effective PCI-mediated gene delivery (Fig. 5).

In *in vitro* experiments, both the ternary complex and the PCI using $AlPcS_{2a}$ showed reduced cell viability as the fluence increased, and the degree of the cytotoxicity depended on the cell lines (Fig. 3a,b, and see Supplementary Information, Figs S1 and S2). Indeed, the PCI conditions have been optimized depending on each cell line[9,10]. However, in this study, a comparison under the same experimental conditions revealed that the ternary complex showed a wider range of safe light doses, in which remarkable enhancement of the transfection was accomplished without reduced cell viability, irrespective of cell lines and incubation time (Fig. 3a and see Supplementary Information, Fig. S2). These results may be due to control of the initial steps in the PCI and highly selective photodamage to the endosomal membrane as described above. We believe that such an expanded range of safe light dose might have resulted in our success in the PCI-mediated gene delivery *in vivo*.

The reduced photocytotoxicity of the ternary complexes might be one of the most important achievements in this study. Because of the pH-dependent membrane binding ability of DPc (Fig. 2b), the photocytotoxicity appears to be reduced when DPc is relocated from the acidic endocytic vesicles into the cytosol. A cytosolic localization of DPc may not be expected to cause the phototoxicity owing to low stability of singlet oxygen in aqueous media. Alternatively, it appears that DPc may undergo slower

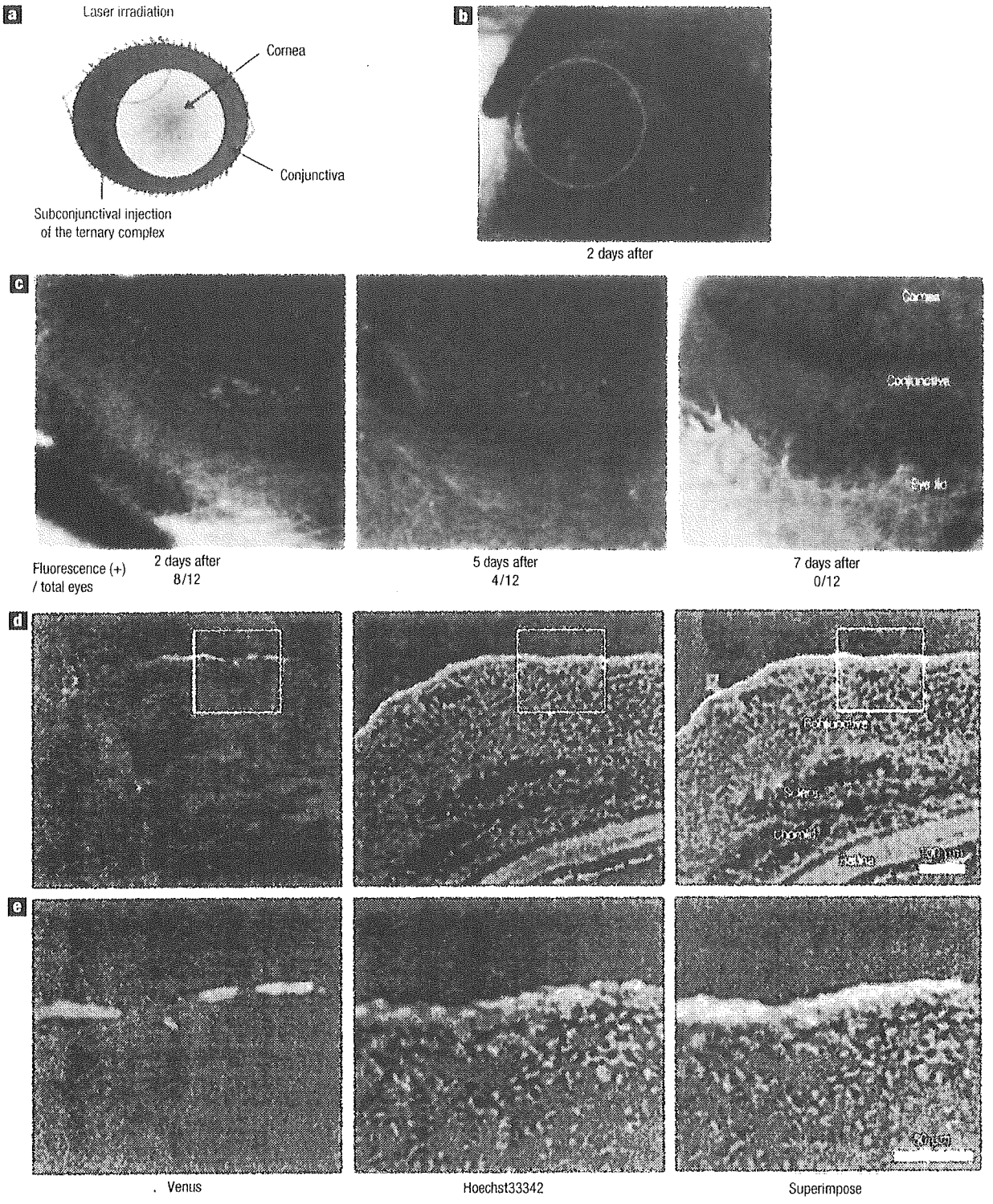

Figure 4 Transfection to the conjunctival tissue to rat eyes. a, The scheme for *in vivo* transfection. Rats were given a subconjunctival injection (coloured in light blue) of each complex containing 15 μg pDNA encoding a variant of a yellow fluorescent protein (Venus). At 2 h post-injection, a part of the conjunctiva (red circle) was irradiated with a light of 689 nm. **b**,**c**, Fluorescent images of the Venus expression in the rat eye at 2, 5 and 7 days after the photochemical transfection using the 1:2:1 ternary complex. The fluorescent-positive eyes/total eyes are indicated below the images. **d**, A fluorescent image of the Venus expression in the frozen section of the conjunctival tissue. The image was taken 2 days after the photochemical transfection using the pDNA/CP_4/DPc 1:2:1 ternary complex. The cell nuclei were stained in blue. **e**, A magnified image of the white square in the above fluorescent image.

diffusion in the cytosol because of its larger size compared with $AlPcS_{2a}$ and have a reduced chance of relocalizing in susceptible cytoplasmic organelles. However, these assumptions remain to be clarified.

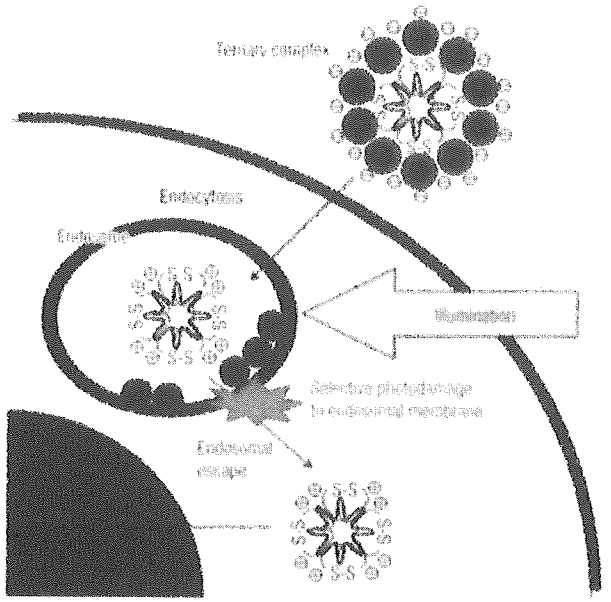

Figure 5 A scheme for itinerary of the ternary complex to the transgene expression. The ternary complex was designed to control the initial steps (that is, internalization by the endocytosis and photodamage of the endosomal membrane to release the polyplex to the cytoplasm) in the PCI-mediated gene delivery.

In the ternary complex system, there is still room for optimization of each component. For example, the polyplex-forming polycations can be optimized, because a variety of polycations can be used for the formation of the ternary complex. Indeed, the ternary complex was formed from poly(L-lysine) at a charge ratio of 1:2:2 (see Supplementary Information, Table S1), and the pDNA/poly(L-lysine)/DPc ternary complex showed approximately 15-fold photochemical enhancement of the transfection with a 50% decrease in the cell viability (see Supplementary Information, Fig. S3). This result suggests that the polyplex-forming polycations significantly affect the transfection efficiency and cytotoxicity, highlighting the importance of optimization of the polycations. In the present study, the CP_4 peptide, of which the nuclear localization and the effective gene transfection following the translocation into the cytoplasm were demonstrated in the previous study[17], was used to prepare the ternary complex, and we successfully obtained the PCI-mediated gene transfection *in vitro* and *in vivo*. Further optimization of the polycations is our future interest, and the studies in this direction will be reported elsewhere.

This system can be potentially useful for the gene therapy of ophthalmic diseases[24]. The molecular design could be expanded to a systemically targeted gene carrier for the treatment of various diseases, including solid tumours. Spatial control of transgene expression in the body will ensure the effectiveness and safety of *in vivo* gene therapy.

METHODS

POLYMER SYNTHESIS AND CHARACTERIZATION

Synthesis of ionic DPc (Fig. 1a) was performed according to the method reported in ref. 25. The detailed synthetic procedure is described in Supplementary Information. The absorption spectra revealed that DPc shows B band absorption at 350 nm and strong Q band absorption at 685 nm.
A cationic peptide $C(YGRKKRRQRRRG)_2$ (CP_2) was synthesized by the Peptide Institute (Osaka, Japan). The CP_4 peptide was prepared by oxidation of the CP_2 peptide in 10 mM of Tris–HCl buffer (pH 7.4) over 14 days. PAA homopolymer (DP: 26; weight-averaged/number-averaged molecular mass (M_w/M_n), 1.2) was synthesized as reported in ref. 26.

PLASMID DNA

A plasmid DNA, pCAcc+Luc, containing a firefly luciferase cDNA driven by a CAG promoter[27] was provided by RIKEN Bioresource Centre (Tsukuba, Japan). Also, a fragment cDNA of SEYFP-F46L (Venus), which is a variant of a yellow fluorescent protein with the mutation F46L[28], was provided by Dr Miyawaki of the Brain Science Institute, RIKEN (Wako, Japan), and inserted into the pCAcc vector (pCAcc+Venus). Each plasmid DNA (pDNA) was amplified in competent DH5α *Escherichia coli* and purified by a HiSpeed Plasmid Maxi Kit (Qiagen, Germany). pCAcc+Luc was used for *in vitro* studies, whereas *in vivo* transfection was performed using pCAcc+Venus.

PREPARATION OF THE TERNARY COMPLEX

The pDNA/CP_4 polyplex was prepared by mixing pDNA and CP_4 peptide in 10 mM of Tris–HCl buffer (pH 7.4) at an N/P ratio of 2 (pDNA concentration, 100 μg ml^{-1}). At 30 min after incubation at ambient temperature, the pDNA/CP_4 polyplex solution was mixed with the DPc solution with varying charge molar ratios of pDNA/CP_4/DPc, followed by an extra 30-min incubation at ambient temperature to obtain the pDNA/CP_4/DPc ternary complex. The ternary complexes with varying ratios of DPc were characterized by a gel retardation assay.

CHARACTERIZATION OF THE TERNARY COMPLEX

The size and polydispersity were evaluated by dynamic light scattering measurement using a DLS-7000 instrument (Otsuka Electronics, Osaka, Japan) equipped with an Ar ion laser (488 nm). The ζ-potential was measured by a laser-Doppler electrophoresis ELS-6000 instrument (Otsuka Electronics) equipped with a He–Ne ion laser (633 nm). AFM imaging was performed in a tapping mode with a standard silicon probe 160 μm in length using an NVB 100 microscope (Olympus, Tokyo, Japan) operated by Nanoscope IIIa software (Digital Instruments, Santa Barbara, California). Detailed experimental conditions are described in Supplementary Information.

OCTANOL/WATER PARTITIONING

The experimental procedure is described in Supplementary Information.

FLOW CYTOMETRY ANALYSIS AND CONFOCAL MICROSCOPIC OBSERVATION

The amount of uptake of each polyplex containing pDNA labelled with fluorescein by HeLa cells was analysed by flow cytometry. The detailed experimental conditions are described in Supplementary Information. Confocal observation of FITC-labelled dextran (M_w: 10,000–15,000) co-incubated with the 1:2:1 ternary complex in HeLa cells before and after photoirradiation was performed using LSM510 (Carl Zeiss, Jena, Germany). Detailed experimental conditions are provided in Supplementary Information.

IN VITRO TRANSFECTION STUDY

HeLa cells (10,000 cells) on a 24-well culture plate were incubated with each polyplex containing 1 μg pDNA in 0.5 ml of DMEM containing 10% FBS, followed by 6- or 24-h incubation and fresh medium replacement. The culture plates were photoirradiated using a 300-W halogen lamp (fluence rate, 3.0 mW cm^{-2}) equipped with a band-pass filter (400–700 nm) with increased fluence (0.9–3.6 J cm^{-2}). After 48 h post-incubation, the transfection efficiency was evaluated by the Luciferase Assay System (Promega, Madison, Wisconsin) and a Lumat LB9507 luminometer (Berthold Technologies, Bad Wildbad, Germany), whereas the cell viability was evaluated by the 3-(4,5-dimethylthiazol-2-yl)-2,5-diphenyltetrazolium bromide (MTT) assay. Sulphonated aluminium phthalocyanine ($AlPcS_{2a}$) and PEI (25 kDa) were purchased from Frontier Scientific (Logan, Utah) and Sigma-Aldrich (St Louis, Missouri), respectively.

IN VIVO TRANSFECTION TO CONJUNCTIVA

Wistar rats (male, 6-weeks old, $n = 12$) (Saitama Experimental Animal Supply, Saitama, Japan) were given a subconjunctival injection of 150 μl of each complex containing 15 μg pDNA (pCAcc+Venus). At 2 h post-injection, the rats were anesthetized and part of the conjunctiva was irradiated using a 689-nm semiconductor laser emitted from in-house built laser equipment (Topcon, Tokyo, Japan) with 2.0 mW laser power and 4 mm projection diameter for 60 s (1 J cm^{-2}). The fluorescent images of the Venus expression in a rat eye and the conjunctival tissues were taken as described in Supplementary Information. All the experimental procedures were handled in accordance with

the guidelines of the Animal Committee of the University of Tokyo. The polyplex from linear PEI, with ExGen500 (Fermentas, Vilnius, Lithuania) as a control vector, was prepared at N/P ratio = 6.

Received 12 July 2005; accepted 28 September 2005; published XX Month XXXX.

References

1. Ogris, M. & Wagner, E. Targeting tumors with non-viral gene delivery systems. *Drug Discov. Today* **7,** 479–485 (2002).
2. Taira, K., Kataoka, K. & Niidome, T. (eds) *Non-viral Gene Therapy: Gene Design and Delivery* (Springer, Tokyo, 2005) (ISBN: 4-431-25122-7).
3. Merdan, T., Kopecek, J. & Kissel, T. Prospects for cationic polymers in gene and oligonucleotide therapy against cancer. *Adv. Drug Deliv. Rev.* **54,** 715–758 (2002).
4. Salem, A. K., Searson, P. C. & Leong, K. W. Multifunctional nanorods for gene delivery. *Nature Mater.* **2,** 668–671 (2003).
5. Behr, J. P. The proton sponge. A trick to enter cells the viruses did not exploit. *Chimia* **51,** 34–36 (1997).
6. Berg, K. *et al.* Photochemical internalization: a novel technology for delivery of macromolecules into cytosol. *Cancer Res.* **59,** 1180–1183 (1999).
7. Høgest, A., Prasmickaite, L., Tjelle, T. E. & Berg, K. Photochemical transfection: A new technology for light-induced, site-directed gene delivery. *Hum. Gene Ther.* **11,** 869–880 (2000).
8. Prasmickaite, L., Høgest, A. & Berg, K. Evaluation of different photosensitizers for use in photochemical gene transfection. *Photochem. Photobiol.* **73,** 388–395 (2001).
9. Høgest, A. *et al.* Photochemical transfection: A technology for efficient light-directed gene delivery. *Somat. Cell Mol. Genet.* **27,** 97–113 (2002).
10. Høgest, A. *et al.* Photochemical internalization in drug and gene delivery. *Adv. Drug Deliv. Rev.* **56,** 95–115 (2004).
11. Macdonald, I. J. & Dougherty, T. J. Basic principle of photodynamic therapy. *J. Porphyrins Phthalocynanines* **5,** 105–129 (2001).
12. Esfand, R. & Tomalia, D. A. Poly(amidoamine) (PAMAM) dendrimers: from biomimicry to drug delivery and biomedical applications. *Drug Discov. Today* **6,** 427–436 (2001).
13. Gillies, E. R. & Frechet, J. M. Dendrimers and dendritic polymers in drug delivery. *Drug Discov. Today* **10,** 35–43 (2005).
14. Duncan, R. The dawning era of polymer therapeutics. *Nature Rev.: Drug Discov.* **2,** 347–360 (2003).
15. Kobayashi, H. *et al.* Lymphatic drainage imaging of breast cancer in mice by micro-magnetic resonance lymphangiography using a nano-size paramagnetic contrast agent. *J. Natl Cancer Inst.* **96,** 703–708 (2004).
16. Tang, M., Redemann, C. T. & Szoka, F. C. Jr. In vitro gene delivery by degraded polyamidoamine dendrimers. *Bioconjugate Chem.* **7,** 703–714 (1996).
17. Rudolph, C. *et al.* Oligomers of the arginine-rich motif of the HIV-1 TAT protein are capable of transferring plasmid DNA into cells. *J. Biol. Chem.* **278,** 11411–11418 (2003).
18. Caruso, F., Caruso, R. A. & Mohnwald, H. Nanoengineering of inorganic and hybrid hollow spheres by colloidal templating. *Science* **282,** 1111–1114 (1998).
19. Donath, E. *et al.* Novel hollow polymer shells by collid-templated assembly of polyelectrolytes. *Angew. Chem. Int. Edn* **37,** 2002–2005 (1998).
20. Levitan, H. & Barker, J. L. Salicylate. Structure-activity study of its effects on membrane permeability. *Science* **176,** 1423–1425 (1972).
21. Itaka, K. *et al.* in *Carrier-Based Drug Delivery* (ed. Svenson, S.) 154–159 (ACS Symp. Series Vol. 879, Americal Chemical Society, 2004).
22. Moan, J., Berg, K., Anholt, A. & Madslien, K. Sulfonated aluminum phthalocyanines as sensitizers for photochemotherapy. Effects of small doses on localization, dye fluorescence and photosensitivity in V79 cells. *Int. J. Cancer* **58,** 865–870 (1994).
23. Rodal, G. H., Rodal, S. K., Moan, J. & Berg, K. Liposome-bound Zn(II)-phthalocyanine. Mechanisms for cellular uptake and photosensitization. *J. Photochem. Photobiol. B* **45,** 150–159 (1998).
24. Daiger, S. P. Was the human genome project worth the efforts? *Science* **308,** 362–364 (2005).
25. Ng, A. C. H., Li, X. & Ng, D. K. P. Synthesis and photophysical properties of nonaggregated phthalocyanines bearing dendritic substitutes. *Macromolecules* **32,** 5292–5298 (1999).
26. Harada, A. & Kataoka, K. Formation of polyion complex micelles in aqueous milieu from a pair of oppositely-charged block copolymers with poly(ethylene glycol) segments. *Macromolecules* **28,** 5294–5299 (1995).
27. Niwa, H., Yamamura, K. & Miyazaki, J. Efficient selection for high-expression transfectants with a novel eukaryotic vector. *Gene* **108,** 193–199 (1991).
28. Nagai, T. *et al.* A variant of yellow fluorescent protein with fast and efficient mutation for cell-biological applications. *Nature Biotechnol.* **20,** 87–90 (2002).

Acknowledgements

We thank N. Kanayama (the University of Tokyo), S. Kawauchi (National Defense Medical College) and K. Date (the University of Tokyo) for technical assistance. This work was supported in part by the Core Research Program for Evolutional Science and Technology (CREST) from Japan Science and Technology Agency (JST).
Correspondence and requests for materials should be addressed to K.K.[3]
Supplementary Information accompanies this paper on www.nature.com/naturematerials.

Competing financial interests

The authors declare that they have no competing financial interests.

46. 眼内血管新生および血管発達における アンジオポイエチン２の作用について

大島裕司[1)]、Peter A Campochiaro[2)]、石橋達朗[1)]
([1)] 九州大、[2)] Johns Hopkins 大)

研究要旨 アンジオポイエチン２(Ang2)は血管内皮細胞を target organ とし血管新生や血管の発育、および血管透過性亢進に関与していることが知られている。今回我々は、眼内血管新生および血管発達における Ang2 の作用について検討した。
Ang2 を強発現する Tet システムを用いたダブルトランスジェニックマウスを作成した(CMV-rtTA/TRE-Ang2)。生直後(P0)より Ang2 を強発現させ P11, P18 に網膜血管の発育を網膜伸展標本および病理組織学的検討を用いて行った。また酸素負荷網膜症モデルを作成し、P7 より Ang2 を強発現、P17 に網膜血管新生について検討した。一部のものについては酸素負荷網膜症モデル作成後、P20 より Ang2 を強発現、P23 に網膜血管新生について検討した。生直後(P0)から Ang2 を強発現させると P11 には網膜深層の血管密度がコントロールに比して有意に高く血管発育が早かったが、P18 には正常密度と同等になり発育を完成した。また酸素負荷網膜症モデルにおいて、網膜虚血の期間に Ang2 を強発現させるとコントロールに比して有意に血管新生促進が認められたが、酸素負荷網膜症を作成後、網膜虚血が改善された時期に Ang2 を強発現させると有意な血管新生抑制が認められた。
Ang2 は眼内の血管発育および血管新生に対して重要な働きをしており、特に成熟していない血管に大きく影響を与えることが示唆された。

A. 研究目的

血管新生は腫瘍増殖、創傷治癒や関節炎など種々の病態において重要な働きを担っており、特に眼内における血管新生は加齢黄斑変性症、糖尿病網膜症や未熟児網膜症の病因となっており、そのメカニズムを解明することは重要である。血管内皮増殖因子(Vascular endothelial cell growth factor; VEGF)ファミリーとそのレセプターは血管新生の主要な働きをしている。しかし、VEGF とそのレセプターの発現や活動性は種々の他の遺伝子産物により制御されている。Tie-2 およびアンジオポイエチン(angiopoietin;Ang)ファミリーや neurophilin などがその代表である。Tie-2 レセプター作用を増強させるナチュラルアゴニストがアンジオポイエチン１(Ang1)であり、その作用をブロックするアンタゴニストがアンジオポイエチン２(Ang2)である。Tie-2 レセプターは血管内皮細胞に特異的に発現し、胎芽の血管発生に重要な働きをしていることが知られており、血管周囲の細胞や細胞外マトリックスに働きかけ、血管を安定化させるのがその主な働きである

と考えられている。Ang2はその働きをブロックするため、VEGFの存在、非存在により異なる働きをすると考えられている。Ang2は血管を非安定化するために、VEGF存在下ではVEGFの作用を増強し、血管新生を促進、VEGF非存在下ではその逆に血管新生を退縮、抑制すると考えられている1)。網膜の正常血管発育および病的網膜血管新生においてAng2の発現は増強していることが報告されている。またAng2の発現が認められないAng2ノックアウトマウスでは、正常でみられる硝子体動脈の退縮が認められないことが報告されている2)。しかし、成熟した網膜血管や成熟したマウスにおける病的新生血管に対するAng2の働きは知られていない。そこで、我々は、
tetracycline-inducible promoter system (Tet system) を用いて成熟網膜血管、網膜血管の正常発達、また病的網膜血管新生におけるAng2の働きについて検討した。

B. 研究方法

1. 実験材料

ドキシサイクリン(DOX) (Sigma, St. Louis USA), fluorescein dextran (Sigma), Superscript preamplification system for first strand cDNA systhesis (Invitrogen, USA), Biotinylatedgriffonia simplicifolia lictin B4(GSA) (Vector Laboratories, USA), HistoMark red(Kirkegaard and Perry, USA), ヤギ抗ヒトVEGF抗体(R&D, USA), ウサギ抗マウスAng2抗体(RDI, USA), Opsin/rtTA-TRE/Ang2ダブルトランスジェニックマウス(Tet/opsin/ang2)、CMV/rtTA-TRE/Ang2ダブルトランスジェニックマウス(Tet/CMV/Ang2)

2. 実験方法

成熟血管に対するAng2の影響

Tet/opsin/ang2ダブルトランスジェニックマウスは生後21日目(P21)に2mg/mlのドキシサイクリン(DOX)を投与する群(DOX+)と投与しない群(DOX-)の二群に分け、DOX+群はDOXを2週間もしくは8週間投与した。その後、眼球摘出、摘出眼は固定後OCTコンパウンドに包埋、薄切を行い病理組織学的検討を行った。また一部の眼球は網膜よりTRIsol(Invitrogen)を用いてRNAを抽出しRT-PCRを行った。

網膜血管発育に対するAng2強発現の影響

Tet/CMV/ang2ダブルトランスジェニックマウスをDOX+とDOX-群に分け、DOX+群には生直後P0より母親マウスに2mg/ml DOXを投与し、P7より児マウスに0.5mg/体重gのDOXを皮下注した。P11およびP18に眼球摘出し、上記と同様に検討した。

酸素負荷網膜症に対するAn2の影響

酸素負荷網膜症モデルはTet/CMV/ang2ダブルトランスジェニックマウスをP7からP12まで75%高濃度酸素を投与することにより作成した。DOX+群はP12より母親マウスに2mg/ml DOXを投与し、P12からP17まで0.5mg/体重gのDOXを皮下注した。P17に眼球摘出、上記と同様に検討した。また一部のものに対しては、酸素負荷網膜症モデル作成後、P20に眼球摘出し、残りの児マウスを二群に分け、DOX+群にはP20からP22まで0.5mg/体重gのDOXを皮下注し、P23に眼球摘出した。

C. 研究結果

成熟血管に対するAng2の影響

DOX 投与によって網膜に Ang2 を過剰発現させた Tet/opsin/ang2 ダブルトランスジェニックマウスおよび Tet/CMV/ang2 ダブルトランスジェニックマウスともに RT-PCR にて網膜に強い RNA の発現が認められ、免疫組織学的にも網膜で Ang2 の強い発現が認められた。しかし、組織学的に網膜血管異常、および機能的に ERG においても異常は認められなかった。

網膜血管発育に対する Ang2 強発現の影響

新生 Tet/CMV/ang2 ダブルトランスジェニックマウスに Ang2 を過剰発現させることによって、P11 において網膜深層血管網の発育がコントロール群に比して明らかに促進されていた。しかし、その後病的な血管発育は認められず、P18 にはコントロール群と同様の血管発育であった。

酸素負荷網膜症に対する An2 の影響

Ang2 を強発現させた DOX+群では P17 において明らかにコントロール群に比して血管新生が促進させていた。また RT-PCR において Ang2 は DOX 群に強く発現しており、VEGF は正常酸素下コントロール比して、DOX+群、DOX-群とも発現が増加していた。

P20 から P23 まで DOX を投与した実験では、Ang2 を強発現させた DOX+群では DOX-群に比べて優位に血管新生を退縮させた。

D. 考察

Tet system を用いて成熟した大人マウスの網膜に Ang2 を過剰発現しても網膜および網膜血管には組織学的にも機能的にも影響を与えなかった。しかし、網膜血管発育途中である児マウスに生直後より Ang2 を強発現すると網膜深層毛細血管網の発育が正常より良好になるが、そのまま強発現を続けても異常血管網とはならず、正常発達が完了しそれ以上の発達は認められなかった。酸素負荷網膜症による網膜新生血管モデルにおいて、VEGF が多く発現している段階では Ang2 は血管新生を促し、逆に VEGF が減少している段階では Ang2 は新生血管を退縮させた。これらのことより、血管にはその発育やその段階、環境によって、Ang2 に対する感受性を支配しているものがあると推察される。発達段階にある網膜深層血管網は Ang2 に対する感受性が高く、そのため、P11 では過剰な Ang2 により血管発達が良好となり、発育が完了した P18 には Ang2 に対する感受性が低くなったと考えられる。また、一旦 Ang2 に対する感受性が高くなった段階で、VEGF が多量に発現すると VEGF による影響を強く受け、特に VEGF/Ang2 の割合が高くなると血管新生に、逆に低くなると新生血管の退縮に働くと推察される。

E. 結論

Ang2 は眼内の血管発育および血管新生に対して重要な働きをしている。将来、Ang2 を VEGF を抑制する薬剤とともに使用することで、眼内血管新生を退縮させ、種々の疾患に対して治療的意義があると推測される。

F. 健康危険情報

なし

G. 研究発表

1. 論文発表

1. Oshima Y et al; Different effects of angiopoietin-2 in different vascular veds in the eye: new vessels are most sensitive. FASEB J. 2005

2. 学会発表

1. Oshima Y et al: Angiopoietin2(Ang2) increases or decreases neovascuralization depending upon the setting. The Association for Research in Vision and Ophthalmology (ARVO), Fort Lauderdale, Florida,2003.

H. 知的財産権の出願・登録状況

1. 特許取得

なし

2. 実用新案登録

なし

3. その他

なし

I. 参考文献

1. Oshima Y et al: Increased Expression of VEGF in Retinal Pigment Epithelial Cells Is not Sufficient to Cause Choroidal Neovascularization. J. Cell. Physiol. 201: 393-400, 2004.
2. Hacett SF et al: Angiopoietin2 expression in the reina: upregulation during physiologic and pathologic neovascularization. J. Cell Physiol.184: 275-284, 2000.

図 1. Tet/CMV/ang2 ダブルトランスジェニックマウスに生後直後より Ang2 を強発現させた網膜深層血管網の面積

P11 には Ang2 強発現群がコントロール群に比して明らかに血管面積が大きかった(＊P<0.01)が、P18 には両者に差は認められなかった。

図 2. P12-P17 に Ang2 を強発現させた酸素負荷網膜症における網膜新生血管面積

Ang2 を強発現させた群が有意にコントロール群に比して面積が大きかった。(＊P<0.01)

図 3. P20-P23 に Ang2 を強発現させた酸素負荷網膜症における網膜新生血管面積

Ang2 を強発現させた群(B, E)がコントロール群(C, F)およびベースライン群(A, D)に比して明らかに網膜新生血管面積が小さかった。(＊P<0.05)

A- F;病理組織学的写真 (GSA 染色)

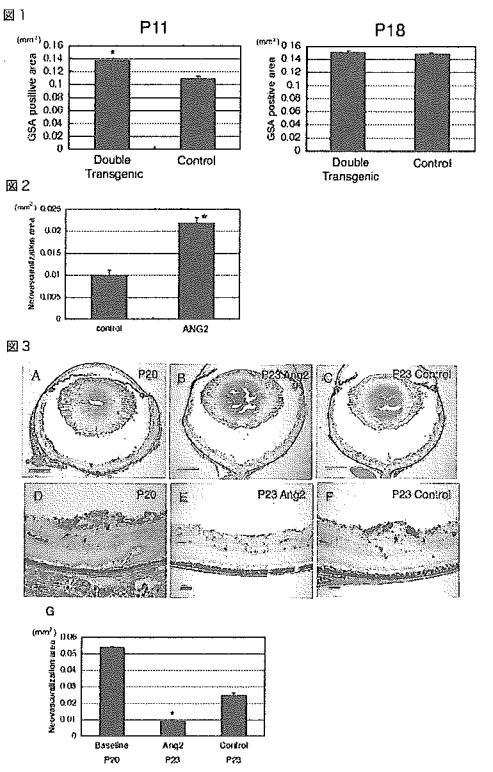

JOURNAL OF CELLULAR PHYSIOLOGY 201:393–400 (2004)

Increased Expression of VEGF in Retinal Pigmented Epithelial Cells Is not Sufficient to Cause Choroidal Neovascularization

YUJI OSHIMA,[1] SACHIKO OSHIMA,[1] HIROYUKI NAMBU,[1] SHU KACHI,[1] SEAN F. HACKETT,[1] MICHELE MELIA,[1] MICHAEL KALEKO,[3] SHEILA CONNELLY,[3] NORIKO ESUMI,[1] DONALD J. ZACK,[1,2] AND PETER A. CAMPOCHIARO[1]*

[1]*The Departments of Ophthalmology and Neuroscience, The Johns Hopkins University School of Medicine, Baltimore, Maryland*
[2]*The Department of Molecular Biology and Genetics, The Johns Hopkins University School of Medicine, Baltimore, Maryland*
[3]*Advanced Vision Therapies, Inc., Rockville, Maryland*

Increased expression of vascular endothelial cell growth factor (VEGF) in the retina is sufficient to stimulate sprouting of neovascularization from the deep capillary bed of the retina, but not the superficial retinal capillaries or the choriocapillaris. Coexpression of VEGF and angiopoietin 2 (Ang2) results in sprouting of neovascularization from superficial and deep retinal capillaries, but not the choriocapillaris. However, retina-derived VEGF and Ang2 may not reach the choriocapillaris, because of tight junctions between retinal pigmented epithelial (RPE) cells. To eliminate this possible confounding factor, we used the human vitelliform macular dystrophy 2 (VMD2) promoter, an RPE-specific promoter, combined with the tetracycline-inducible promoter system, to generate double transgenic mice with inducible expression of VEGF in RPE cells. Adult mice with increased expression of VEGF in RPE cells had normal retinas and choroids with no choroidal neovascularization (CNV), but when increased expression of VEGF in RPE cells was combined with subretinal injection of a gutless adenoviral vector containing an expression construct for Ang2 (AGVAng2), CNV consistently occurred. In contrast, triple transgenic mice with induced expression of Ang2 and VEGF in RPE cells, did not develop CNV. These data suggest that increased expression of VEGF and/or Ang2 in RPE cells is not sufficient to cause CNV unless it is combined with a subretinal injection of a gutless adenoviral vector, which is likely to perturb RPE cells. These data also suggest that the effects of angiogenic proteins may vary among vascular beds, even those that are closely related, and, therefore, generalizations should be avoided. J. Cell. Physiol. 201: 393–400, 2004.

Neovascularization plays an important role in many disease processes such as tumor growth, arthritis, atherosclerosis, proliferative retinopathies, and age-related macular degeneration. Understanding the molecular signals involved in neovascularization would greatly facilitate the development of new treatments for these disease processes. However, it is unlikely that there is a single cascade of signals that is responsible for neovascularization in all vascular beds and all disease processes. On the other hand, it is equally unlikely that there is no overlap in the molecular pathogenesis of new vessel growth in different vascular beds. To explore this issue, it is necessary to compare the effects of angiogenic and antiangiogenic proteins in several well-characterized vascular beds.

The eye is advantageous for studies of this type. The transparency of the cornea, lens, and vitreous allows direct visualization of retinal vessels and some visualization of the choroidal vessels in living animals. This is aided by intravascular injection of fluorescent dyes, which enhance resolution of retinal and choroidal vessels and help to assess vascular permeability. In

Contract grant sponsor: The National Eye Institute; Contract grant numbers: EY05951, EY12609, P30EY1765; Contract grant sponsor: Research to Prevent Blindness; Contract grant sponsor: Foundation Fighting Blindness.

*Correspondence to: Peter A. Campochiaro, Maumenee 719, The Johns Hopkins University School of Medicine, 600 N. Wolfe Street, Baltimore, MD 21287-9277. E-mail: pcampo@jhmi.edu

Received 21 November 2003; Accepted 27 January 2004

DOI: 10.1002/jcp.20110

the eye, there are several vascular beds separated by avascular tissue, so effects on multiple vascular beds can be studied. Vascular invasion of adjacent avascular tissue provides unequivocal identification of neovascularization and the absence of background vessels facilitates quantification. Cell type-specific promoters provide powerful tools that allow production of proteins at various locations within the eye to assess their effects on the various vascular beds (Okamoto et al., 1997; Ohno-Matsui et al., 2002).

We first employed this strategy by coupling the rhodopsin promoter to a full-length cDNA for the 165 amino acid isoform of vascular endothelial cell growth factor (VEGF) to generate transgenic mice with increased expression of VEGF in photoreceptors (Okamoto et al., 1997). These mice had increased production of VEGF specifically in photoreceptors starting on postnatal day (P) 7, and shortly thereafter developed sprouting of new vessels from the deep capillary bed of the retina, but not the superficial retinal or choroidal vessels. In a follow-up study, we utilized the tetracycline-inducible promoter system to generate double transgenic mice with inducible expression of VEGF in photoreceptors (Ohno-Matsui et al., 2002). Initiation of VEGF expression in photoreceptors in adult mice also caused neovascularization originating only from deep retinal capillaries, but if VEGF expression was initiated between P0 and P7, sprouting occurred from the superficial as well as the deep capillaries (Oshima et al., 2003a). Angiopoietin 2 (Ang2) is expressed along the surface of the retina between P0 and P7, but beyond P7 it is expressed in the region of the deep capillary bed (Hackett et al., 2000). We, therefore, examined the effect of coexpression of VEGF and Ang2. Double transgenic mice with doxycycline-inducible expression of Ang2 were given an intravitreous injection of a gutless adenoviral vector containing an expression construct for VEGF and then treated with doxycycline or not treated with it. Those treated with doxycycline expressed both VEGF and Ang2, and developed retinal neovascularization, while those that were not treated, expressed only VEGF and did not develop retinal neovascularization (Oshima et al., 2003a). Therefore, coexpression of Ang2 is required for retinal vessels to sprout new vessels in response to VEGF.

Coexpression of VEGF and Ang2 in the retina did not cause choroidal neovascularization (CNV). One possible explanation is that increased levels of VEGF and Ang2 are not sufficient to stimulate CNV, but an alternative explanation is that the tight junctions between retinal pigmented epithelial (RPE) cells prevent retina-derived VEGF and Ang2 from reaching choroidal vessels. In this study, we circumvented the second possibility by using the RPE-specific, human vitelliform macular dystrophy 2 (VMD2) promoter (Esumi et al., 2003) to drive expression of VEGF and Ang2 in RPE cells and thereby test the effect of VEGF and Ang2 on choroidal vessels.

MATERIALS AND METHODS

Generation of VMD2 promoter/reverse tetracycline transactivator (VMD2/rtTA) transgenic mice

A plasmid pUHD172-1neo, which contains the gene encoding rtTA (Gossen et al., 1995), was kindly provided by Dr. Manfred Gossen (University of Heidelberg, Germany). The −585 to +38 bp fragment of human VMD2 (Esumi et al., 2003), was selected to drive expression in RPE cells. The 1 kb rtTA cDNA was released from pUHD172-1neo by digestion with EcoR I/BamH I, gel-purified, blunt-ended, and ligated into the placF vector downstream of the VMD2 promoter (this resulted in loss of the LacZ cassette) (Esumi et al., 2003). The VMD2/rtTA fragment was then digested by Kpn I/Bgl II, gel-purified to remove vector sequence, and microinjected into mouse one-cell embryos (B6/SJL F2 hybrid) at the Transgenic Mouse Core Facility of Johns Hopkins University School of Medicine. Mouse pups born from several different microinjections were screened by polymerase chain reaction (PCR) of tail DNA with transgene-specific primers (forward: 5′-TTA CGG GTC TAC CAT CGA GG-3′; reverse: 5′-GCG AGA TGC TCT TGA AGT CT-3′). Two VMD2/rtTA transgenic founders were obtained and mated with C57BL/6 mice to generate two transgenic lines. Mice from each of these lines were crossed with tetracycline response element (TRE)/VEGF transgenic mice that have been previously described (Ohno-Matsui et al., 2002). Offspring were screened by PCR using the primers listed above to identify the VMD2/rtTA transgene, and the primers used to identify the TRE/VEGF transgene were (forward: 5′-TCG ACT AGG CGT GTA CGG-3′; reverse: 5′-GCA GCA GCC CCC GCA TCG-3′).

Triple transgenic mice with inducible expression of VEGF and Ang2 in RPE cells

Mice from a double transgenic line with inducible expression of VEGF in RPE cells, VMD2/rtTA-TRE/VEGF (Tet/VMD2/VEGF), were crossed with TRE/Ang2, line 5 mice (Oshima et al., 2003b). Primers used to identify the TRE/Ang2 transgene (forward: 5′-GTG AAA GTC GAG CTC GGT-3′; reverse: 5′-TGT TGA CGG TCT CCA TTA GG-3′) amplify a specific 1,144 bp product.

Production of gutless adenoviral vectors (AGV) encoding Ang2

The procedures for generation of AGV encoding Ang2 are very similar to those previously described (Oshima et al., 2003c). Briefly, all gutless vector plasmids used to generate AGV contained the left and the right ITRs flanked by unique Pac I sites, the packaging signal of type 5 adenovirus, and human alpha synuclein intronic region as a stuffer sequence (Reddy et al., 2002). The cDNA encoding human Ang2 under control of the cytomegalovirus (CMV) immediate-early enhancer/promoter and the SV40 late polyadenylation signal was inserted into the polylinker region of pCI (Promega, Madison, WI), to generate pCIAng2. The Ang2 expression cassette from pCIAng2 was then introduced into the Pme I site present in the polylinker of a shuttle plasmid, pGTI.24aPL2 to generate pGTI24-Ang2. The plasmid, pGTI.24aPL2, contains a polylinker flanked by human alpha synuclein DNA (Zerby et al., 2003). To generate the gutless vector plasmid, pGTI24-Ang2 was digested with Pac I to liberate the plasmid backbone and combined with Pme I/Mlu I-digested pBV4. The plasmid pBV4 contains 27,191 bp of human alpha synuclein stuffer DNA (Zerby et al., 2003).

Generation of AGVAng2 from plasmid, large-scale vector production, and purification were performed as

described (Reddy et al., 2002). The particle titers were evaluated by optical density measurements, and AGVAng2 vector titer was 7.9×10^{11} particles/ml. DNA extracted from the purified AGVAng2 vector was analyzed by restriction enzyme digestion and did not show any detectable rearrangements. A hexon-based quantitative PCR assay was used to determine the level of helper virus contamination in gutless vector preparation (Reddy et al., 2002), and contamination levels were less than 1%.

RT-PCR

Adult double transgenic mice were given drinking water containing 2 mg/ml of doxycycline and 5% glucose. After 2 weeks, mice were euthanized, eyes were removed, and total RNA was isolated with TRIzol reagent (Invitrogen, Carlsbad, CA) following the manufacturer's instructions. Reverse transcription was carried out with 1.0 μg of total RNA, SuperScript II reverse transcriptase (Invitrogen), and 5.0 μM oligo (dT) primer. Aliquots of the cDNAs were used for PCR amplification using primers that specifically amplify a 380 bp fragment of human VEGF (forward: 5′-CAC CCA TGG CAG AAG GAG GAG-3′; reverse: 5′-CAA ATG CTT TCT CCG CTC TGA-3′) or a 438 bp fragment of murine Ang2 (forward: 5′-AGA TCC AAC AGA ATG TGG TGC-3′; reverse: 5′-TGT TGA CGG TCT CCA TTA GG-3′). Titrations were performed to ensure that PCR reactions were carried out in the linear range of amplification. Mouse S16 ribosomal protein primers (forward: 5′-CAC TGC AAA CGG GGA AAT GG-3′; reverse: 5′-TGA GAT GGA CTG TCG GAT GG-3′) were used to provide an internal control for the amount of template in the PCR reactions.

Histochemistry and immunohistochemistry

Mice were euthanized and eyes were fixed in 4% paraformaldehyde in 0.05 M phosphate-buffered saline (PBS) for 1 h and rinsed twice in 25% sucrose in PBS. Specimens were incubated in 25% sucrose in PBS overnight and embedded in optimal cutting temperature embedding compound (OCT; Miles Diagnostics, Elhart, IN). Ocular frozen sections (10 μm) were histochemically stained with biotinylated Griffonia simplicifolia lectin B4 (GSA; Vector Laboratories, Burlingame, CA), which selectively binds to vascular cells, as previously described (Ozaki et al., 1998). Briefly, slides were incubated in methanol/H_2O_2 for 10 min at 4°C, washed with 0.05 M Tris-buffered saline, pH 7.6 (TBS), and incubated for 30 min in 10% normal porcine serum. Slides were incubated for 2 h at room temperature with biotinylated GSA and after rinsing with 0.05M TBS, they were incubated with streptavidin-phosphatase and developed with HistoMark Red (Kirkegaard and Perry, Gaithersburg, MD). Sections were rinsed in TBS and deionized water, and dehydrated by passing them through a step gradient consisting of 70, 95, and 100% ethanol, and xylene. Sections were mounted with Cytoseal XYL mounting medium (Richard-Alan Scientific, Kalamazoo, MI), examined with a Nikon microscope, and captured as digital files with a Nikon Digital Still Camera DXM1200 (Nikon Instruments, Inc., NY).

To stain for human VEGF, ocular frozen sections were dried with cold air for 5 min, fixed in freshly prepared 4% paraformaldehyde in 0.05 M PBS at 4°C for 30 min, and rinsed with TBS for 10 min. Endogenous peroxidases were blocked by a 10 min incubation with 0.75% H_2O_2 in PBS. Slides were washed three-times in H_2O and once with 0.01 M citrate buffer, and then with warm citrate buffer. The sections were heated in a microwave for 1 min after onset of the boiling of the buffer. After cooling for 1 min, sections were blocked with 1% skim milk in TBS for 1 h at room temperature. Sections were incubated overnight at 4°C in 1:10 polyclonal goat anti-human VEGF (R&D Systems, Minneapolis, MN). After two rinses in TBS, sections were incubated for 30 min at room temperature with 1:200 biotinylated bovine anti-goat IgG (Santa Cruz Biotechnology, Inc., Santa Cruz, CA). After washing, slides were incubated in streptavidin-phosphatase, developed with HistoMark Red, and mounted as described above.

To stain for murine Ang2, sections were incubated in a 1:50 dilution consisting of 20 μg/ml rabbit anti-mouse Ang2 (Research Diagnostics, Inc., Flanders, NJ) in blocking solution overnight at 4°C. After two rinses in TBS, sections were incubated for 30 min at room temperature with 1:200 biotinylated goat anti-rabbit IgG (Vector Laboratories). After a wash, slides were incubated in streptavidin-phosphatase, developed with HistoMark Red, and mounted.

Injection of vectors

Mice were treated humanely in strict compliance with the Association for Research in Vision and Ophthalmology statement on the use of animals in research. Intraocular injections of vector were done as previously described (Mori et al., 2001). Briefly, adult Tet/VMD2/VEGF double transgenic mice were treated with 2 mg/ml of doxycycline in their drinking water for 2 weeks and then given a subretinal injection of 1×10^8 viral particles of AGVAng2 in one eye and a subretinal injection of 1×10^8 viral particles of AGVNull in the other eye. Injections were done with a Harvard pump microinjection apparatus and pulled glass micropipets. Each micropipet was calibrated to deliver 1 μl of vehicle upon depression of a foot switch. The mice were anesthetized, pupils were dilated, and a fragment of a coverslip was used as a contact lens under a dissecting microscope to visualize the retina. The sharpened pipet tip was passed through the sclera just posterior to the limbus and positioned above the retina. Depression of the foot switch caused the jet of injected fluid to penetrate the retina and detach roughly ½ of the retina. After subretinal injections, mice were treated with 2 mg/ml of doxycycline in their drinking water for an additional 2 weeks and then anesthetized. Retinas were examined using a dissecting microscope with a fragment of a coverslip as a contact lens. Fundus pictures were taken using a digital camera (Nikon coolpix 990; Nikon Instruments, Inc.).

Fluorescein angiography

Mice were anesthetized and 2 min after intraperitoneal injection of 12 μl/g body weight of 1% fluorescein sodium (Alcon, Fort Worth, TX), the retinas were examined with a fluorescence microscope (Axioskop, Zeiss, Thornwood, NY). Images were digitized with a 3 color CCD video camera (IK-TU40A, Toshiba, Tokyo, Japan) and a frame grabber.

Assessment of neovascularization

Mice were anesthetized and perfused with 1 ml of PBS containing 50 mg/ml of fluorescein-labeled dextran (2×10^6 average molecular weight, Sigma, St. Louis, MO) as previously described (Tobe et al., 1998). Eyes were removed and fixed for 1 h in 10% phosphate-buffered formalin. Corneas were removed, retinas were carefully dissected, and four radial cuts were made in eyecups to allow flat mounting (AquaPolyMount, Polysciences, Warrington, PA). The area of CNV at Bruch's membrane rupture sites was measured by image analysis using Image-Pro Plus software (Media Cybernetics, Silver Spring, MD).

RESULTS

Double transgenic mice with doxycycline-inducible expression of VEGF in RPE cells

Two VMD2/rtTA transgenic founders were obtained and crossed with C57BL/6 mice to obtain two independent transgenic lines. Mice from each of the lines were crossed with TRE/VEGF transgenic mice that had been previously characterized (Ohno-Matsui et al., 2002). One line of double hemizygous VMD2/rtTA-TRE/VEGF (Tet/VMD2/VEGF) mice showed no detectable expression of human VEGF mRNA in total RNA isolated from whole eye when not treated with doxycycline (DOX−), but when given 2 mg/ml of doxycycline (DOX+) for 2 weeks, there was strong expression of human VEGF mRNA (Fig. 1). This high level of VEGF mRNA expression was maintained after 4 weeks of doxycycline treatment, the longest time point examined. Double hemizygous Tet/VMD2/VEGF mice generated from the second VMD2/rtTA transgenic line showed substantial expression of human VEGF mRNA when not treated with doxycycline (not shown), and, therefore, this line of mice was eliminated.

Increased expression of VEGF in RPE cells for up to 4 weeks does not cause CNV

Double hemizygous Tet/VMD2/VEGF mice were randomly assigned to DOX− or DOX+ groups. After 2 or 4 weeks, ocular sections stained with the vascular cell marker GSA showed completely normal superficial, intermediate, and deep capillary beds and no ectopic retinal vessels nor CNV (Fig. 2). This indicates that increased expression of VEGF in RPE cells for up to 4 weeks does not cause CNV.

Increased expression of VEGF and Ang2 in RPE cells does not cause CNV

We have recently generated TRE/Ang2 transgenic mice in which a murine Ang2 cDNA is coupled to the TRE (Oshima et al., 2003b). Double hemizygous DOX+ rhodopsin promoter/rtTA-TRE/Ang2 (Tet/Opsin/Ang2) mice express high levels of Ang2 in the retina, which increases the sensitivity of retinal vessels to VEGF. To test if Ang2 increases the sensitivity of choroidal vessels to VEGF, we generated triple hemizygous Tet/VMD2/VEGF/Ang2 mice. Using primers specific for human VEGF or murine Ang2, RT-PCR demonstrated that DOX+ Tet/VMD2/VEGF/Ang2 mice had high levels of human VEGF and murine Ang2 mRNA in the eye (Fig. 3). Ocular sections stained with GSA from triple hemizygous Tet/VMD2/VEGF/Ang2 mice that were treated with doxycycline for 2 (Fig. 4A) or 4 weeks (Fig. 4D) demonstrated normal retinal vessels and no evidence of CNV. Some of these mice had hypopigmented RPE cells, making it possible to visualize staining for Ang2 (Fig. 4B) and VEGF (Fig. 4C) in the RPE of DOX+ Tet/VMD2/VEGF/Ang2 mice.

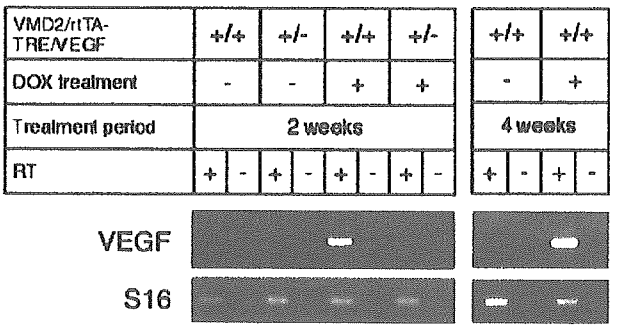

Fig. 1. Doxycycline-induced expression of human vascular endothelial cell growth factor (VEGF) mRNA in the eyes of double transgenic Tet/vitelliform macular dystrophy 2 (VMD2)/VEGF mice. Adult double transgenic Tet/VMD2/VEGF mice or mice carrying only one of the transgenes were given 2 mg/ml of doxycycline in their drinking water for 2 or 4 weeks and then euthanized. Total RNA was extracted from whole eyes and RT-PCR was done using primers specific for human VEGF. In the absence of doxycycline, there was no detectable expression of VEGF mRNA in mice carrying one or both transgenes. Treatment with doxycycline for 2 weeks resulted in prominent expression of VEGF mRNA in double transgenic mice, but not mice carrying only one of the transgenes. The expression was maintained at a comparable level after treatment of double transgenics with doxycycline for 4 weeks.

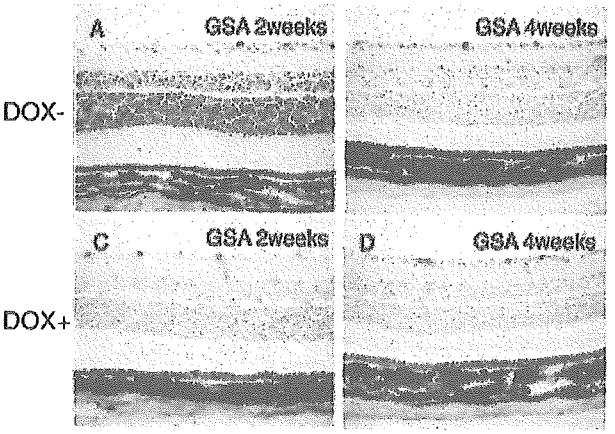

Fig. 2. Treatment of Tet/VMD2/VEGF mice with doxycycline for 2 or 4 weeks does not cause choroidal neovascularization (CNV) or any other identifiable changes in the retina. Adult Tet/VMD2/VEGF mice were treated with 2 mg/ml of doxycycline in their drinking water (DOX+) or given unsupplemented water (DOX−) and euthanized after 2 or 4 weeks. Ocular frozen sections were stained with Griffonia simplicifolia lectin (GSA), which selectively stains vascular cells, and counterstained with hematoxylin. In both DOX+ (C, D) and DOX− (A, B) mice, there were normal appearing retinal vessels and no ectopic vessels in the outer retina or subretinal space.

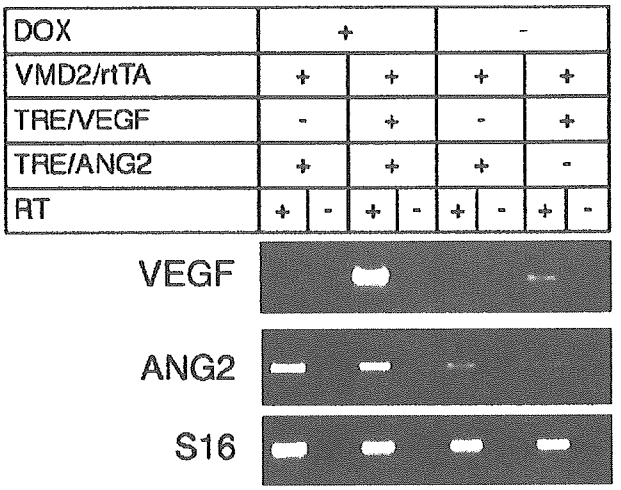

Fig. 3. Triple transgenic Tet/VMD2/VEGF/angiopoietin 2 (Ang2) mice express high levels of VEGF and Ang2 mRNA in the eye when treated with doxycycline. Mice carrying the VMD2/reverse tetracycline transactivator (rtTA) transgene and one or both of the TRE/VEGF and TRE/Ang2 transgenes were given 2 mg/ml of doxycycline in their drinking water (DOX+) or unsupplemented water (DOX−). Double transgenic Tet/VMD2/Ang2 mice expressed high levels of murine Ang2 mRNA in the presence of doxycycline and low levels typical of endogenous expression in the absence of doxycycline. With or without doxycycline, there was no detectable expression of human VEGF mRNA. Double transgenic Tet/VMD2/VEGF mice expressed basal levels of murine Ang2 mRNA and low-level human VEGF mRNA (mild leakiness) in the absence of doxycycline. Triple transgenic Tet/VMD2/VEGF/Ang2 mice treated with doxycycline expressed high levels of human VEGF and murine Ang2 mRNA.

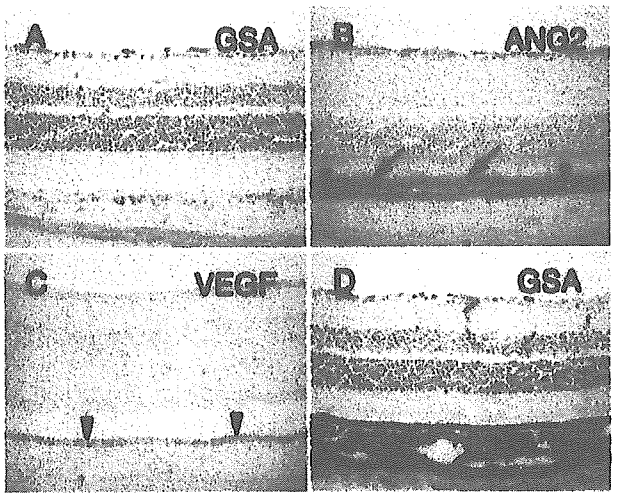

Fig. 4. Treatment of Tet/VMD2/VEGF/Ang2 mice with doxycycline for 2 or 4 weeks does not cause CNV or any other identifiable changes in the retina. Adult lightly pigmented (A–C) Tet/VMD2/VEGF/Ang2 mice or the same triple transgenics in a C57BL6 background (D) were treated with 2 mg/ml of doxycycline in their drinking water and euthanized after 2 (A–C) or 4 weeks (D). Ocular frozen sections stained with GSA, which selectively stains vascular cells, show normal retinal vessels and no ectopic vessels in the outer retina or subretinal space (A and D). The GSA binding was visualized with HistoMark Red and the sections were counterstained with hematoxylin, so that blood vessels appear red and the nuclei of retinal neurons are blue. Immunohistochemical staining for Ang2 using HistoMark Red shows strong staining for Ang2 in retinal pigmented epithelial (RPE) cells (B, arrowheads) and between photoreceptor outer segments (arrows). Immunohistochemical staining for VEGF shows staining in RPE cells (C, arrowheads).

Subretinal injection of AGVAng2 in DOX+ Tet/VMD2/VEGF mice causes CNV

We have previously demonstrated that subretinal injection of gutless adenoviral vectors containing an expression construct for β-galactosidase or endostatin results in high-level expression of these transgenes in RPE cells (Takahashi et al., 2003; Oshima et al., 2003a). Double hemizygous DOX+ Tet/VMD2/VEGF mice were given a subretinal injection of 1×10^8 particles of AGVAng2 in one eye and 1×10^8 particles of AGVNull in the other eye. Two weeks after injection, eyes injected with AGVAng2 showed fluid and blood beneath the retina (Fig. 5A) and fluorescein angiography demonstrated hyperfluorescent areas (Fig. 5B). The hyperfluorescent areas increased in size with increasing time after injection of fluorescein, which is indicative of leakage of dye from CNV. In contrast, eyes injected with AGVNull had normal funduscopic examinations or showed small areas of whitening beneath the retina (Fig. 5C) and normal fluorescein angiograms or small areas of hyperfluorescence (Fig. 5D). Choroidal flat mounts after perfusion with fluorescein-labeled dextran showed large areas of CNV in all six eyes that had been injected with AGVAng2 (Fig. 5E), while four of six eyes that had been injected with AGVNull showed small areas of CNV (Fig. 5F). Measurement of CNV areas by image analysis showed that the average area of CNV per eye was significantly greater in eyes injected with AGVAng2 compared to those injected with AGVNull (Fig. 5E).

In many eyes of double hemizygous DOX+ Tet/VMD2/VEGF mice that were given a subretinal injection of AGVAng2, there were multiple areas of CNV with some remote from the injection site, but still within the area of the subretinal bleb (Fig. 6A,B), suggesting that the perturbation of the RPE caused by the subretinal injection was not simply due to mechanical damage at the injection site. These eyes showed strong staining for Ang2 in RPE cells throughout the region of the subretinal bleb (Fig. 6C, arrowheads) and also showed strong staining for VEGF in CNV (Fig. 6D,E, arrows) and RPE cells (Fig. 6E, arrowheads). Inflammatory cells were not noted. The fellow eye of that shown in Figure 6A–E was injected with AGVNull and showed no detectable CNV beneath the injection site (Fig. 6F, arrows) or elsewhere.

DISCUSSION

In this study, we used the tetracycline-inducible promoter system to induce expression of VEGF in RPE cells of adult mice and found that this was not sufficient to cause CNV. Using the same system to induce expression of both VEGF and Ang2 in RPE cells, we found that this also was insufficient to cause CNV. However, doxycycline-induced expression of VEGF in RPE cells combined with subretinal injection of a gutless adenoviral vector containing an expression cassette for

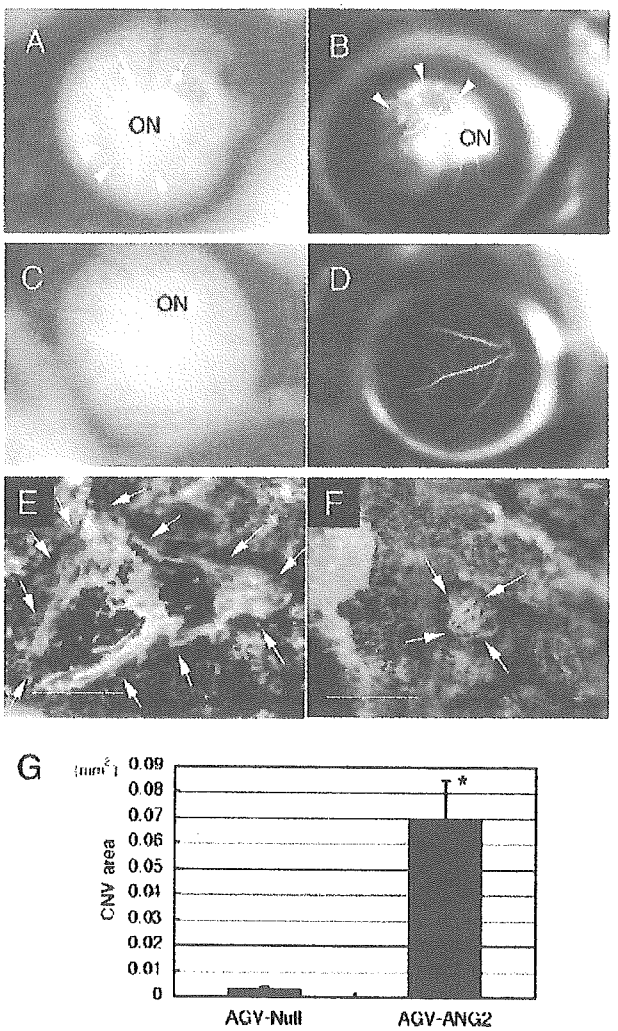

Fig. 5. Treatment with doxycycline and subretinal injection of AGVAng2 results in severe CNV in Tet/VMD2/VEGF mice. Adult Tet/VMD2/VEGF mice were treated with 2 mg/ml of doxycycline (DOX+) in their drinking water and were given a subretinal injection of 1×10^8 particles of AGVAng2 (A, B, E) or AGVNull (C, D, F). Two weeks after injection of AGVAng2, funduscopic examination showed areas of whitening (A, arrows) around the optic nerve (ON) with adjacent blood (arrowheads) beneath the retina. Fluorescein angiography in another DOX+ Tet/VMD2/VEGF mouse injected with AGVAng2 showed an area of leakage of dye (arrow) adjacent to the ON (B). The arrowheads in B outline subretinal accumulation of dye corresponding to subretinal fluid. Two weeks after injection of AGVNull in a DOX+ Tet/VMD2/VEGF mouse, funduscopic examination showed a small area of whitening (C, arrow) below the ON. Fluorescein angiography in a similarly treated mouse appeared normal except for a small area of hyperfluorescence (D). Choroidal flat mounts of DOX+ Tet/VMD2/VEGF mice perfused with fluorescein-labeled dextran 2 weeks after subretinal injection of AGVAng2, showed large areas of CNV (E, arrows). In contrast, mice injected with AGVNull showed small areas of CNV (F, arrows). Measurement by image analysis of the area of CNV on choroidal flat mounts after fluorescein dextran perfusion in DOX+ Tet/VMD2/VEGF mice showed a significantly larger mean area of CNV in AGVAng2-injected eyes ($n = 6$) compared to AGVNull-injected eyes ($n = 6$) (G). $^*P = 0.0039$ by Mann–Whitney U-test.

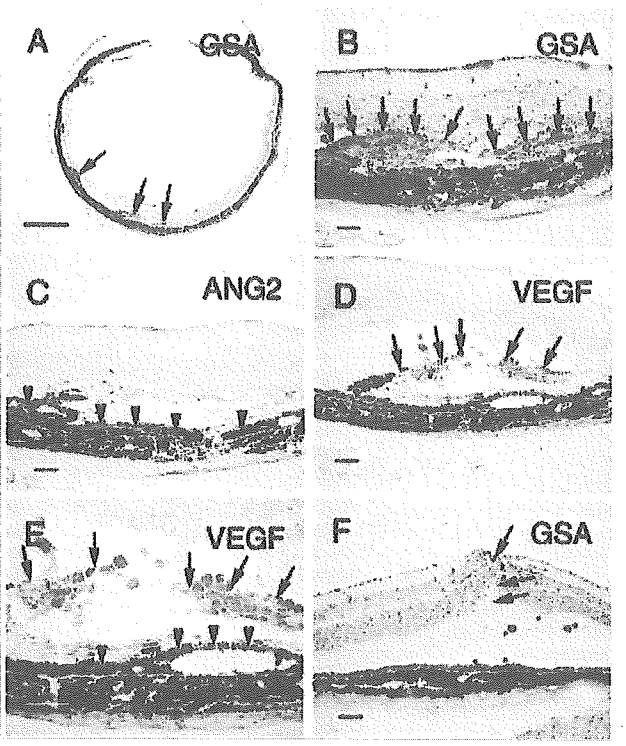

Fig. 6. High expression of Ang2 and VEGF, and severe CNV in eyes of doxycycline-treated Tet/VMD2/VEGF mice after injection of AGVAng2. Sections of eyes of doxycycline-treated Tet/VMD2/VEGF mice after injection of AGVAng2 stained with GSA and counterstained with hematoxylin showed multiple large areas of CNV (A and B, arrows). Immunohistochemical staining for Ang2 showed staining in RPE cells (C, arrowheads). Staining for VEGF showed staining in vascular cells in CNV lesions (D and E, arrows) and in RPE cells (E, arrowheads). In the fellow eye that was injected with AGVNull, staining with GSA showed no CNV beneath the site of injection (F, arrows) or elsewhere in the eye.

Ang2, caused multiple large areas of CNV. Four of six eyes expressing VEGF in RPE cells that received a subretinal injection of empty vector also developed small areas of CNV, but the total area of CNV per eye was significantly less than that seen in eyes injected with AGVAng2. These results suggest that several molecular signals are required for blood vessels to sprout from choroidal vessels and penetrate Bruch's membrane.

Increased expression of VEGF in the skin of transgenic mice using a keratin promoter is sufficient to stimulate neovascularization (Thurston et al., 1999). Increased expression of VEGF in the retina stimulates neovascularization from the deep retinal capillary bed, but not from superficial retinal capillaries, unless the increased expression of VEGF occurs between postnatal day (P) 0 and P7, in which case new vessels sprout from superficial retinal vessels (Okamoto et al., 1997; Oshima et al., 2003a). These observations point out two concepts that are underemphasized in the angiogenesis literature. (1) Different vascular beds differ with regard to the way they respond to "angiogenic factors." (2) The same vascular bed can differ in its response to "angiogenic factors" at different times during development. A likely

explanation is that the expression of gene products that modulate the effects of a particular "angiogenic factor" may differ in and around different vascular beds and in the same vascular bed at different times during development. This concept is supported by the demonstration that Ang2 is expressed in the region of the superficial capillary bed of the retina between P0 and P7, when the superficial capillaries are responsive to VEGF, but not later in life when responsiveness to VEGF is lost (Hackett et al., 2000). Furthermore, coexpression of high levels of Ang2 and VEGF stimulates neovascularization from the superficial retinal vessels (Oshima et al., 2003b). For choroidal vessels, coexpression of VEGF and Ang2 in RPE cells is not sufficient to stimulate CNV, but CNV can occur when increased expression of VEGF in RPE cells is combined with subretinal injection of a viral vector, and in this setting the amount of CNV is markedly increased by expression of Ang2. It is not clear what action of viral vectors injected into the subretinal space facilitates the occurrence of CNV in the presence of high expression of VEGF in RPE cells, but some possibilities include induction of expression of a cytokine(s) that increases sensitivity to VEGF, induction of expression of VEGF receptors, or perturbation of RPE cells resulting in reduction of an inhibitory factor that normally suppresses the effect of VEGF. The observation that subretinally injected viral vectors facilitate the development of CNV may explain why subretinal injection of viral vectors encoding VEGF causes CNV (Baffi et al., 2000; Spilsbury et al., 2000; Wang et al., 2003), while induced expression of VEGF in RPE cells of transgenic mice does not cause CNV.

Transgenic mice in which the murine Rpe65 promoter drives expression of VEGF in RPE cells show a thickened choroid (Schwesinger et al., 2001). Despite up to 4 weeks of increased expression of VEGF in RPE cells of adult mice, we did not observe any thickening of the choroid. Expression of Rpe65 begins early in development. Therefore, a likely explanation for the difference between our results and those of Schwesinger et al. (2001) is that increased expression of VEGF in RPE cells early in development stimulates the developmental growth of choroidal vessels resulting in thickening of the choroid. This is analogous to the stimulation of growth of superficial retinal vessels when VEGF is expressed in the retina between P0 and P7 (Oshima et al., 2003a).

In summary, there is some feature of the microenvironment of choroidal vessels that differs from that retinal vessels or vessels in skin, and prevents increased levels of VEGF and Ang2 from stimulating CNV. It may be that a cytokine that is constitutively expressed in retina and skin is not expressed in choroid unless it is induced by subretinal injection of a viral vector or laser-induced rupture of Bruch's membrane (Yamada et al., 2000). Alternatively, the RPE and Bruch's membrane may provide a mechanical and/or biochemical barrier that prevents increased expression of VEGF and Ang2 in RPE cells from stimulating CNV. The barrier could be constituted by an inhibitory factor(s) present in the RPE and/or Bruch's membrane, such as TIMP3 or PEDF, which are present in high levels in both tissues. If this is the case, the effect of a subretinal injection of viral vector or laser-induced rupture of Bruch's membrane (Yamada et al., 2000) may be to cause a localized area where levels of inhibitory factors are decreased. Additional studies are needed to determine between these possibilities and if the latter possibility is correct, to characterize the nature of the barrier, which could provide the basis for a treatment to prevent CNV in disease states such as age-related macular degeneration.

ACKNOWLEDGMENTS

This study is supported by grants from The National Eye Institute (core grant P30EY1765) and Research to Prevent Blindness (a Lew R. Wasserman Merit Award, to P.A.C.; a Senior Investigator Award, to D.J.Z.; an unrestricted grant). P.A.C. is the George S. and Dolores Dore Eccles Professor of Ophthalmology. D.J.Z. is the Guerrieri Professor of Ophthalmology.

LITERATURE CITED

Baffi J, Byrnes G, Chan C-C, Csaky KG. 2000. Choroidal neovascularization in the rat induced by adenovirus mediated expression of vascular endothelial growth factor. Invest Ophthalmol Vis Sci 41: 3582–3589.

Esumi N, Oshima Y, Li Y, Campochiaro PA, Zack DJ. 2004. Analysis of the VMD2 promoter and implication of E-box binding factors in its regulation. J Biol Chem 279:19064–19073.

Gossen M, Freundlieb S, Bender G, Muller G, Hillen W, Bujard H. 1995. Transcriptional activation by tetracyclines in mammalian cells. Science 268:1766–1769.

Hackett SF, Ozaki H, Strauss RW, Wahlin K, Suri C, Maisonpierre P, Yancopoulos G, Campochiaro PA. 2000. Angiopoietin 2 expression in the retina: Upregulation during physiologic and pathologic neovascularization. J Cell Physiol 184:275–284.

Mori K, Duh E, Gehlbach P, Ando A, Takahashi K, Pearlman J, Mori K, Yang HS, Zack DJ, Ettyreddy D, Brough DE, Wei LL, Campochiaro PA. 2001. Pigment epithelium-derived factor inhibits retinal and choroidal neovascularization. J Cell Physiol 188:253–263.

Ohno-Matsui K, Hirose A, Yamamoto S, Saikia J, Okamoto N, Gehlbach P, Duh EJ, Hackett SF, Chang M, Bok D, Zack DJ, Campochiaro PA. 2002. Inducible expression of vascular endothelial growth factor in photoreceptors of adult mice causes sever proliferative retinopathy and retinal detachment. Am J Pathol 160:711–719.

Okamoto N, Tobe T, Hackett SF, Ozaki H, Vinores MA, LaRochelle W, Zack DJ, Campochiaro PA. 1997. Transgenic mice with increased expression of vascular endothelial growth factor in the retina: A new model of intraretinal and subretinal neovascularization. Am J Pathol 151:281–291.

Oshima Y, Oshima S, Takahashi K, Nambu H, Apte RS, Duh E, Hackett SF, Zack DJ, Campochiaro PA. 2003. Angiopoietin 2 (Ang2) increases or decreases neovascularization depending upon the setting. Invest Ophthalmol Vis Sci 44:4519 E-abstract.

Oshima Y, Deering T, Oshima S, Nambu H, Reddy PS, Kaleko M, Connelly S, Hackett SF, Campochiaro PA. 2004a. Angiopoietin-2 enhances retinal vessel sensitivity to vascular endothelial growth factor. J Cell Physiol 199:412–417.

Oshima Y, Takahashi K, Oshima S, Saishin Y, Saishin Y, Silva RL, Liang X, Reddy PS, Ganesh S, Brann R, Liau G, Kaleko M, Connelly S, Campochiaro PA. 2004b. Intraocular gutless adenoviral vectored VEGF stimulates anterior segment but not retinal neovascularization. J Cell Physiol 199:399–411.

Ozaki H, Okamoto N, Ortega S, Chang M, Ozaki K, Sadda S, Vinores MA, Derevjanik N, Zack DJ, Basilico C, Campochiaro PA. 1998. Basic fibroblast growth factor is neither necessary nor sufficient for the development of retinal neovascularization. Am J Pathol 153: 757–765.

Reddy PS, Sakhuja K, Ganesh S, Yang L, Kayda D, Brann T, Pattison S, Golightly D, Idamakanti N, Pinkstaff A, Kaloss M, Barjot C, Chamberlain JS, Kaleko M, Connelly S. 2002. Sustained human factor VIII expression in hemophilia A mice following systemic delivery of a gutless adenoviral vector. Molec Ther 5:63–73.

Schwesinger C, Yee C, Rohan RM, Joussen AM, Fernandez A, Meyer TN, Poulaki V, Ma JJK, Redmond TM, Liu S, Adamis AP, D'Amato RJ. 2001. Intrachoroidal neovascularization in transgenic

mice overexpressing vascular endothelial growth factor in the retinal pigment epithelium. Am J Pathol 158:1161–1172.
Spilsbury K, Garrett KS, Shen WY, Constable IJ, Rakoczy PE. 2000. Overexpression of vascular endothelial growth factor (VEGF) in the retinal pigment epithelium leads to the development of choroidal neovascularization. Am J Pathol 157:135–144.
Takahashi K, Saishin Y, Saishin Y, Lima Silva R, Oshima Y, Oshima S, Melia M, Paszkiet B, Zerby D, Kadan MJ, Liau G, Kaleko M, Connelly S, Luo T, Campochiaro PA. 2003. Intraocular expression of endostatin reduces VEGF-induced retinal vascular permeability, neovascularization, and retinal detachment. FASEB J 17:896–898. Epub 2003 Mar 28.
Thurston G, Suri C, Smith K, McClain J, Sato TN, Yancopoulos GD, McDonald DM. 1999. Leakage-resistant blood vessels in mice transgenically overexpressing angiopoietin-1. Science 286:2511–2515.
Tobe T, Okamoto N, Vinores MA, Derevjanik NL, Vinores SA, Zack DJ, Campochiaro PA. 1998. Evolution of neovascularization in mice with overexpression of vascular endothelial growth factor in photoreceptors. Invest Ophthalmol Vis Sci 39:180–188.
Wang F, Rendahl KG, Manning WC, Quiroz D, Coyne M, Miller SS. 2003. AAV-mediated expression of vascular endothelial growth factor induces choroidal neovascularization in rat. Invest Ophthalmol Vis Sci 44:781–790.
Yamada H, Yamada E, Kwak N, Ando A, Suzuki A, Esumi N, Zack DJ, Campochiaro PA. 2000. Cell injury unmasks a latent proangiogenic phenotype in mice with increased expression of FGF2 in the retina. J Cell Physiol 185:135–142.
Zerby D, Sakhuja K, Reddy PS, Zimmerman H, Kayda D, Ganesh S, Pattison S, Brann T, Kadan MJ, Kaleko M, Connelly S. 2003. In vivo ligand-inducible regulation of gene expression in a gutless adenoviral vector system. Hum Gene Ther 14:749–761.

47. 軸索を再生したネコ網膜神経節細胞における ON-中心型／OFF-中心型細胞の不均衡

矢田崇晋[1)]、中村　誠[1)]、寺崎浩子[1)]、渡部眞三[2)]
([1)]名古屋大、[2)]発達障害研究所)

研究要旨　視神経切断後末梢神経を断端に移植すると、網膜神経節細胞の軸索が再生してくる。しかし、再生した視神経細胞のON細胞の占める割合が、OFF細胞のそれより大きい。我々は再生細胞数を増加させることによって、ON細胞とOFF細胞が均等に軸索を再生するかどうか調べた。その結果、緑内障の治療薬である、ニプラジロールが均衡に軸索を再生させることが分かった。

A．研究目的

ほ乳動物視神経の切断端に末梢神経を移植すると、移植神経内に軸索が再生する。しかし、軸索を再生したネコ網膜神経節細胞（RGC）ではON細胞が多数を占めると報告され、正常網膜でのON／OFF細胞の割合と異なっている。このため再生視神経による視機能の回復には、再生細胞数の増加だけでなくON／OFF細胞の割合の不均衡の是正も重要である。我々は再生細胞数を増加させた場合のON／OFF細胞の割合を調べた。

B．研究方法

ネコの視神経切断端に総腓骨神経片を自家移植し、6週後に移植神経に蛍光色素を注入して、再生細胞を標識した。標識された細胞内にLuciffer Yellowを注入して、樹状突起の形態を明らかにし、樹状突起の形態から細胞のタイプを分類した。免疫染色によりINL層とIPL層の境界線を可視化し、樹状突起のIPL層における分枝からON細胞とOFF細胞を識別した。再生細胞数を増加させるために、視神経切断前に神経栄養因子、あるいはnipradilolを眼球内に注入した。また、一部の動物は暗闇で飼育して、軸索再生に及ぼす光刺激遮断の効果を調べた。動物はすべて笑気-ハロセンの吸入麻酔によって麻酔し、実験は無菌条件で行うとともに、必要に応じて抗生物質を投与した。実験後、動物はネンブタールの過剰投与で安楽死させた。

C．研究結果

正常網膜：我々の方法ではON細胞、OFF細胞がそれぞれ58%対42%と、ほぼ等しい割合となった。軸索再生：生理食塩水を注入した網膜（control）においては74%対26%とON細胞の割合が優位に増加していた。軸索再生促進：神経栄養因子（BDNF + CNTF + forskolin）を眼球内に注入すると、再生細胞数が増加する。しかし神経栄養因子注入では、88%対12%とON細胞の割合がさらに増加していた。Nipradilolを眼球内に注入した場合でも再生細胞数が増加するが、57%

対 43%で正常網膜に近い割合となった。光刺激遮断下での軸索再生：移植後暗闇で飼育した網膜においては、ON 細胞と OFF 細胞は 79%対 21%で、control 群と比べて優位な OFF 細胞の増加は見られなかった。

D．考察

末梢神経移植による RGC の軸索再生能は、ON 細胞において高いことを示した。神経栄養因子注入は主に再生 ON 細胞を増加させるが、Nipradilol 注入は ON 細胞と OFF 細胞のいずれの再生細胞も増加させた。再生時光刺激遮断は OFF 細胞の増加に関与していないことが分かった。

E．結論

軸索を再生した RGC において、ON 細胞数が大きかった。ニプラジロールは網膜神経節細胞の ON 細胞と OFF 細胞の軸索を均等に再生させる。

F．健康危険情報

なし

G．研究発表

1．論文発表

なし

2．学会発表

神経の再生移植学会

1. 矢田 崇晋他：軸索を再生した網膜神経節細胞の *a* 亜層細胞と *b* 亜層細胞の割合. 神経の成長・再生・移植研究会第 20 回学術集会、吹田市、2005
2. 矢田 崇晋他：軸索を再生ネコ網膜神経節細胞における ON-中心型/OFF-中心型細胞の不均衡.第 9 回視覚フォーラム、弘前市、2005

H．知的財産権の出願・登録状況

1．特許取得

なし

2．実用新案登録

なし

3．その他

なし

I．参考文献

1. Wässle H et al: Morphology and topography of on-and off-alpha cells in the cat retina. Proc R Soc London ;B212: l57-175, 1981.
2. Wässle H et al: Morphology and mosaic of on-and off-beta cells in the cats retina and some functional considerations. Proc R Soc London ;B212: l77-195, 1981.
3. Watanabe, M et al: Proportions of ON center versus OFF center Cells in Retinal Ganglion Cells with Regenerated Axons of Adult Cats. Experimental neurology 143: 117-123, 1997.
4. Watanabe,M et al: Environmental Light Enhances Survival and Axonal Regeneration of Axotomized Retinal Ganglion Cells in Adult Cats. Experimental Neurology 160: 133-141, 1999.
5. Miyoshi. T et al: Receptive-field properties of adult cats retinal ganglion cells with regenerated axons .Exp Brain Res. 125: 383-390,

1999.

6. Watanabe, M et al: Intravitreal injection of neurotrophic factors and forskolin enhance survival and axonal regeneration of axotomized β ganglion cells in cat retina. Neuroscience 116: 733-742, 2003.
7. Watanabe, M et al.: Anti-Glaucoma Drug, Nipradilol at Low Concentration Promotes Regeneration of Retinal Ganglion Cells in Adult Cats. 投稿中

Neuroscience 116 (2003) 733–742

INTRAVITREAL INJECTIONS OF NEUROTROPHIC FACTORS AND FORSKOLIN ENHANCE SURVIVAL AND AXONAL REGENERATION OF AXOTOMIZED β GANGLION CELLS IN CAT RETINA

M. WATANABE,[a]* Y. TOKITA,[b] M. KATO[a] AND Y. FUKUDA[c]

[a]*Department of Physiology, Institute for Developmental Research, Kasugai, 480-0392 Aichi, Japan*

[b]*Department of Perinatology, Institute for Developmental Research, Kasugai, 480-0392 Aichi, Japan*

[c]*Department of Physiology and Biosignaling, Osaka University Medical School, Suita, 565-0871 Osaka, Japan*

Abstract—Some retinal ganglion cells in adult cats survive axotomy for two months and regenerate their axons when a peripheral nerve is transplanted to the transected optic nerve. However, regenerated retinal ganglion cells were fewer than 4% of the total retinal ganglion cell population in the intact retina. The present study examined the effects of intravitreal injections of neurotrophic factors (brain-derived neurotrophic factor, ciliary neurotrophic factor, basic fibroblast growth factor, glial cell-derived neurotrophic factor, neurotrophin 4), first on the survival of axotomized cat retinal ganglion cells within 2 weeks, and then on axonal regeneration of the retinal ganglion cells for 2 months after peripheral nerve transplantation. We tested first enhancement of the survival by one of the factors, and then one or two of them supplemented with forskolin, which increases intracellular cAMP. Single injections of 0.5 μg or 1 μg brain-derived neurotrophic factor, 1 μg ciliary neurotrophic factor, or 1 μg glial cell-derived neurotrophic factor significantly increased total numbers of surviving retinal ganglion cells; 1.6–1.8 times those in control retinas. Identification of retinal ganglion cell types with Lucifer Yellow injections revealed that the increase of surviving β cells was most conspicuous: 2.5-fold (brain-derived neurotrophic factor) to 3.6-fold (ciliary neurotrophic factor). A combined injection of 1 μg brain-derived neurotrophic factor, 1 μg ciliary neurotrophic factor, and 0.1 mg forskolin resulted in a 4.7-fold increase of surviving β cells, i.e. 50% survival on day 14. On the axonal regeneration by peripheral nerve transplantation, a combined injection of brain-derived neurotrophic factor, ciliary neurotrophic factor, and forskolin resulted in a 3.4-fold increase of β cells with regenerated axons. The increase of regenerated β cells was mainly due to the enhancing effect of neurotrophic factors on their survival, and possibly to a change of retinal ganglion cell properties by cAMP to facilitate their axonal regeneration. © 2003 IBRO. Published by Elsevier Science Ltd. All rights reserved.

Key words: retinal ganglion cell, survival after axotomy, BDNF, CNTF, cAMP, transplantation.

Axotomized retinal ganglion cells (RGCs) can survive and regenerate their axons when a peripheral nerve (PN) segment is transplanted to the stump of the optic nerve (ON) (Aguayo, 1985; So and Aguayo, 1985). We have been studying axonal regeneration of cat RGCs, taking advantage of well-established classification based on their morphological and physiological characteristics. Our previous works revealed that dendritic morphology of the majority of regenerated cat RGCs is comparable to that of normal α and β cells, with some exceptions named "unclassified" (Watanabe et al., 1991; Watanabe et al., 1993). We further recorded single unit activities from regenerated RGC axons, and found that 95% of regenerated RGCs retain visual response properties of normal Y- and X-cells, physiological counterparts of α and β cells, respectively (Miyoshi et al., 1999). These results imply that cat RGCs not only maintain their original dendritic configurations but also function to transmit visual information even after axotomy and axonal regeneration (Watanabe et al., 1997; Fukuda et al., 1998).

Despite long survival and axonal regeneration of axotomized cat RGCs, the number of regenerated RGCs is still less than 4% of the total population in the cat retina (Watanabe et al., 1993), being small in number for substantial recovery of impaired vision. Further, because β cells occupy the largest population in the central retina and can detect a small visual object, their survival and axonal regeneration is essential for functional recovery of acute vision. In the previous study on cat RGCs with regenerated axons, we found that Y/α cells have higher regeneration ability than X/β and non-α/β (NAB) cells (Watanabe et al., 1993). To understand the mechanism underlying the different ability in axonal regeneration, we then investigated the survival time course of each cell type after ON transection. We found that within 14 days, more than 90% of β cells died, whereas 35% of α cells died (Watanabe et al., 2001), implying that β cells are more susceptible to axonal injury than α cells. Therefore, some means should be established to promote β cell survival for the recovery of acute vision.

The first purpose of the present study was to examine how much survival of axotomized cat RGCs is enhanced by intravitreal injections of neurotrophic factors which re-

*Corresponding author. Tel: +81-568-880811 ext. 3542; fax: +81-1568-880829.
E-mail address: mwatan@inst-hsc.pref.aichi.jp (M. Watanabe).

Abbreviations: BDNF, brain-derived neurotrophic factor; B+C+f, brain-derived neurotrophic factor + ciliary neurotrophic factor + forskolin; CNTF, ciliary neurotrophic factor; DiI, 1,1'-dioctadecyl-3,3,3',3'-tetramethylindocarbocyanine perchlorate; FGF2, basic fibroblast growth factor; GDNF, glial cell-derived neurotrophic factor; LY, Lucifer Yellow; MAG, myelin-associated glycoprotein; NAB, non-α/β cell; NGF, nerve growth factor; NT-4, neurotrophin 4; ON, optic nerve; PN, peripheral nerve; RGCs, retinal ganglion cells; R/S ratio, regeneration/survival ratio.

0306-4522/03$30.00+0.00
doi:10.1016/S0306-4522(02)00562-6